

# Genomic Characterization of Chromosomal Insertions: Insights into the Mechanisms Underlying Chromothripsis

Takema Kato<sup>a</sup> Yuya Ouchi<sup>a,b</sup> Hidehito Inagaki<sup>a,b</sup> Yoshio Makita<sup>g</sup>  
Seiji Mizuno<sup>c</sup> Mitsuharu Kajita<sup>d</sup> Toshiro Ikeda<sup>e</sup> Kazuhiro Takeuchi<sup>f</sup>  
Hiroki Kurahashi<sup>a,b</sup>

<sup>a</sup>Division of Molecular Genetics, Institute for Comprehensive Medical Science (ICMS), and <sup>b</sup>Genome and Transcriptome Analysis Center, Fujita Health University, Toyoake, <sup>c</sup>Department of Pediatrics, Central Hospital, Aichi Human Service Center, Kasugai, <sup>d</sup>Department of Pediatrics, Toyota Kosei Hospital, Toyota, <sup>e</sup>Department of Obstetrics and Gynecology, Faculty of Medicine, Kagoshima University, and <sup>f</sup>Takeuchi Ladies Clinic/Infertility Center, Kagoshima, and <sup>g</sup>Education Center, Asahikawa Medical University, Hokkaido, Japan

## Keywords

Chromothripsis · Insertion · Trisomy rescue

## Abstract

Chromosomal insertions are rare structural rearrangements, and the molecular mechanisms underlying their origin are unknown. In this study, we used whole genome sequencing to analyze breakpoints and junction sequences in 4 patients with chromosomal insertions. Our analysis revealed that none of the 4 cases involved a simple insertion mediated by a 3-chromosomal breakage and rejoining events. The inserted fragments consisted of multiple pieces derived from a localized genomic region, which were shuffled and rejoined in a disorderly fashion with variable copy number alterations. The junctions were blunt ended or with short microhomologies or short microinsertions, suggesting the involvement of nonhomologous end-joining. In one case, analysis of the parental origin of the chromosomes using nucleotide varia-

tions within the insertion revealed that maternal chromosomal segments were inserted into the paternal chromosome. This patient also carried both maternal alleles, suggesting the presence of zygotic trisomy. These data indicate that chromosomal shattering may occur in association with trisomy rescue in the early postzygotic stage.

© 2017 S. Karger AG, Basel

Chromosomal structural rearrangements (CSRs), also known as gross chromosomal rearrangements, are generated by 2 double-strand DNA breaks (DSBs) followed by aberrant DNA repair [Shaffer and Lupski, 2000; Kurahashi et al., 2009]. The DSBs are generally processed by an error-free pathway, called homologous recombination, and repaired properly. However, recurrent CSRs are

T.K. and Y.O. contributed equally to this work.

caused by genomic instability induced by 2 specific sequences that exist as DSB hotspots [Kato et al., 2012]. Alternatively, DSBs at the segmental duplications are often repaired aberrantly by nonallelic homologous recombination (NAHR), leading to recurrent CSRs [Ou et al., 2011; Hermetz et al., 2012]. In contrast, DSBs that arise randomly are often repaired by an error-prone pathway, nonhomologous end-joining (NHEJ), which leads to nonrecurrent CSRs [Gu et al., 2008]

Recent advances in genomic analysis have provided detailed information on the breakpoints and junction sequences of CSRs and have helped us to understand their origin and mechanism. We now know that replication-based pathways such as fork-stalling and template-switching as well as microhomology-mediated break-induced replication are the major pathways leading to CSRs [Zhang et al., 2009]. The products of these pathways occasionally manifest complex junction structures that include duplication or triplication of the breakpoint proximity. In addition, recent high-resolution microarray and next-generation sequencing studies have found that large numbers of complex chromosomal rearrangements occur in one or a few chromosomes [Holland and Cleveland, 2012]. This catastrophic rearrangement is called chromothripsis. Unfortunately, the precise mechanism that induces the chromosome shattering is still unknown [Kloosterman et al., 2011; Stephens et al., 2011].

Chromosomal insertion, also called insertional translocation, is one of several gross interchromosomal structural rearrangements [Van Hemel and Eussen, 2000]. Insertions involve a translocation of a segment from one chromosome and its insertion as an interstitial region into another nonhomologous chromosome [Weckselblatt and Rudd, 2015]. Balanced carriers are healthy but occasionally have reproductive problems such as infertility, recurrent pregnancy loss, or offspring with multiple congenital anomalies due to an unbalanced insertion. Unbalanced insertions also arise *de novo*. They are relatively rare CSRs, with an estimated incidence of about 1:80,000 according to conventional cytogenetic techniques [Van Hemel and Eussen, 2000]. However, 3 recent cohort studies using high-resolution aCGH in conjunction with FISH found a higher incidence than previously estimated [Kang et al., 2010; Neill et al., 2011; Nowakowska et al., 2012].

Little is known about the mechanism of the insertion. It requires at least 3 breaks followed by aberrant repair, but information on the breakpoints and junctions is scarce. One previous study using microarray analysis showed that a small subset of insertions may involve the

NAHR pathway, but the etiology of most nonrecurrent insertions is unclear [Neill et al., 2011]. A recent large-scale study using next-generation sequencing of 6 cases with an insertion identified the underlying mechanism leading to the insertion to be a chromothripsis-like replication-related pathway [Gu et al., 2016]. In the present study, we characterized 4 insertion cases via a combination of cytogenetic and genomic techniques such as whole genome sequencing and mate-pair sequencing for the detection of rearrangement breakpoints. We subsequently genotyped the polymorphisms on the relevant chromosomes and determined their parental origin, thereby shedding light on the mechanisms underlying the origin of the insertion.

## Case Reports and Results

### Case 1

This patient was referred to our facility because of developmental delay. Initial G-banding revealed a 46,XX,add(14)(q32.1) karyotype. We performed cytogenetic microarray analysis and detected a duplication in chromosome 4q and a deletion in 14q. Detailed copy number analysis revealed complex chromosomal rearrangements that included duplications encompassing a 13.1-Mb region at 4q32.1q32.3 and a 0.3-Mb region in 4q35.2, some parts of which appeared to be triplicated, while a 2.7-Mb deletion was found in 14q32.33 (Fig. 1a). Subsequently, using FISH, we found that these copy number variations were due to a chromosomal insertion of 4q32.1q32.3 into 14q32.33 (Fig. 1b). This insertion was not identified in either of the parents and was found to have occurred *de novo* in the index case.

Next, we performed whole genome sequencing to determine the breakpoints and junctions. LUMPY, a probabilistic structural variant caller, revealed the presence of 6 discordant reads, possibly including the junctions of the rearrangements. To characterize breakpoints at a nucleotide resolution, breakpoint-spanning PCR followed by Sanger sequencing was performed. According to the sequence information of the 6 junctions, the original fragments were shuffled and rejoined in a disorderly manner (Fig. 1c). Some regions were lost, while some appeared twice among the inserted fragments, resulting in triplication. Of the junction sequences identified, 1 involved simple end-joining (junction 1), 2 had microhomology of a few nucleotides (junctions 3 and 6), and 1 had a 4-nucleotide microinsertion (junction 1). The remaining 2 junctions carried insertions consisting of small pieces of a segment derived from the vicinity of the breakpoint region in chromosome 4 (Fig. 1d; junctions 4 and 5). The likely structure is shown in Figure 1d, e.

To determine the parental origin of the chromosomal insertion, we genotyped common SNPs in the related regions of chromosomes 4 and 14 using DNA from the proband and his parents. When we compared the SNP data of the 14q32.33 region deleted in the proband, the proband carried only the maternal allele, supposedly reflecting the normal homolog of chromosome 14. This suggests that the original chromosome 14 of *der*(14) with the insertion was of paternal origin (Fig. 1f). Following, we genotyped

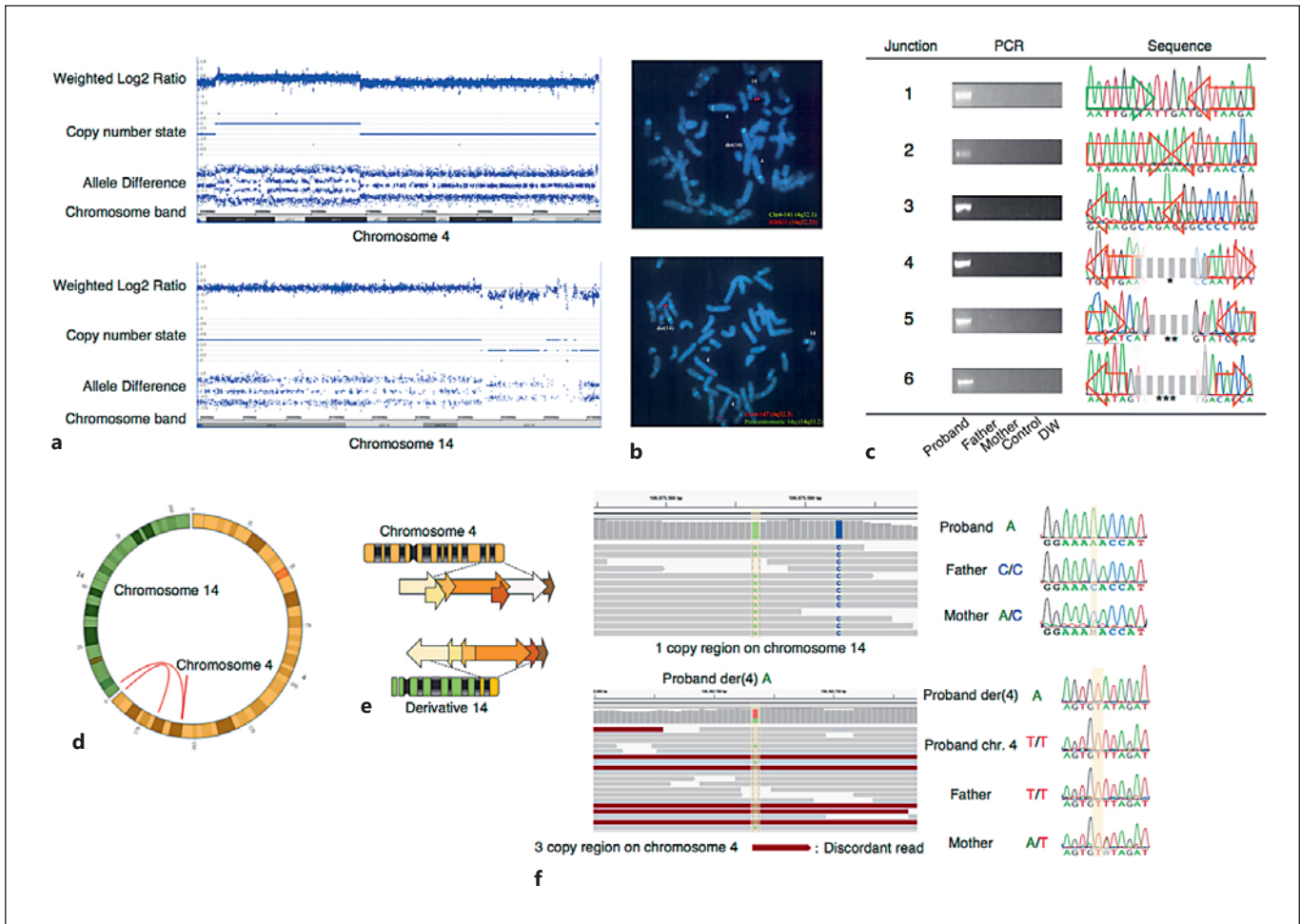


**Fig. 1.** Analysis of the chromosomal insertion in case 1. **a** Chromosome Analysis Suite (ChAS) graphic results for chromosomes 4 and 14 showing copy number gain and loss, respectively. The results are designated as  $\text{arr}[\text{hg}19] \ 4\text{q}32.1\text{q}32.3(156,376,846-169,441,822) \times 3 \sim 4, 4\text{q}35.2(190,659,209-190,957,473) \times 3, 14\text{q}32.33(104,549,511-107,285,437) \times 1$ . Although ChAS showed a normal copy number region within the deletion in chromosome 14, FISH analysis did not identify it as a diploid region (data not shown). **b** FISH confirming the deletion in 14q32.33 (red) shown at the top and the insertion of 4q32.3 (red) into the long arm of chromosome 14 (green) shown at the bottom. **c** Breakpoint-specific PCR and its sequence. Green and orange arrows indicate chromosomes 14 and 4, respectively. The distance between the arrows correlates with microhomology or microinsertion. Asterisks indicate the insertion of a few dozen nucleotides. \* The gray-dashed line encompasses a 35-nt sequence at position

156,671,582–156,671,616 in chromosome 4 and a 37-nt sequence of unknown origin. \*\* The gray-dashed line encompasses a 24-nt sequence of unknown origin, a 21-nt sequence at position 156,711,369–156,711,389 in chromosome 4 with inverted orientation, and a 34-nt sequence of unknown origin. \*\*\* The gray-dashed line encompasses a 25-nt sequence of unknown origin. **d** The detected chromosomal rearrangements are visualized by a Circos plot using ClicO FS. **e** Multiple segments in chromosome 4 were shuffled and inserted into chromosome 14. Some of the segments were missing or duplicated during the rearrangements. **f** An example of a parent-of-origin analysis. The top shows the vicinity of the breakpoint, and the bottom shows a deleted region in chromosome 14. Discordant reads (dark red) and SNPs (light green and blue) are visualized by different colors. SNP genotyping was conducted by Sanger sequencing. SNPs are superimposed on the yellow background.

the SNPs within the insertional region in chromosome 4. The inserted segments were found to originate from the maternal chromosome. This indicates a postzygotic origin of the insertion. Furthermore, the proband was found to have 2 normal chromosomes 4, one paternal and the other maternal, and this normal maternal chromosome 4 was revealed to be a different allele from

the inserted segments of maternal origin. Thus, it is suggested that 2 normal chromosomes 4 were transmitted from the mother and one from the father and that one of the maternal chromosomes 4 was then shattered and integrated into the paternal chromosome 14 in the early postzygotic stage in the trisomic zygote (Fig. 5a).



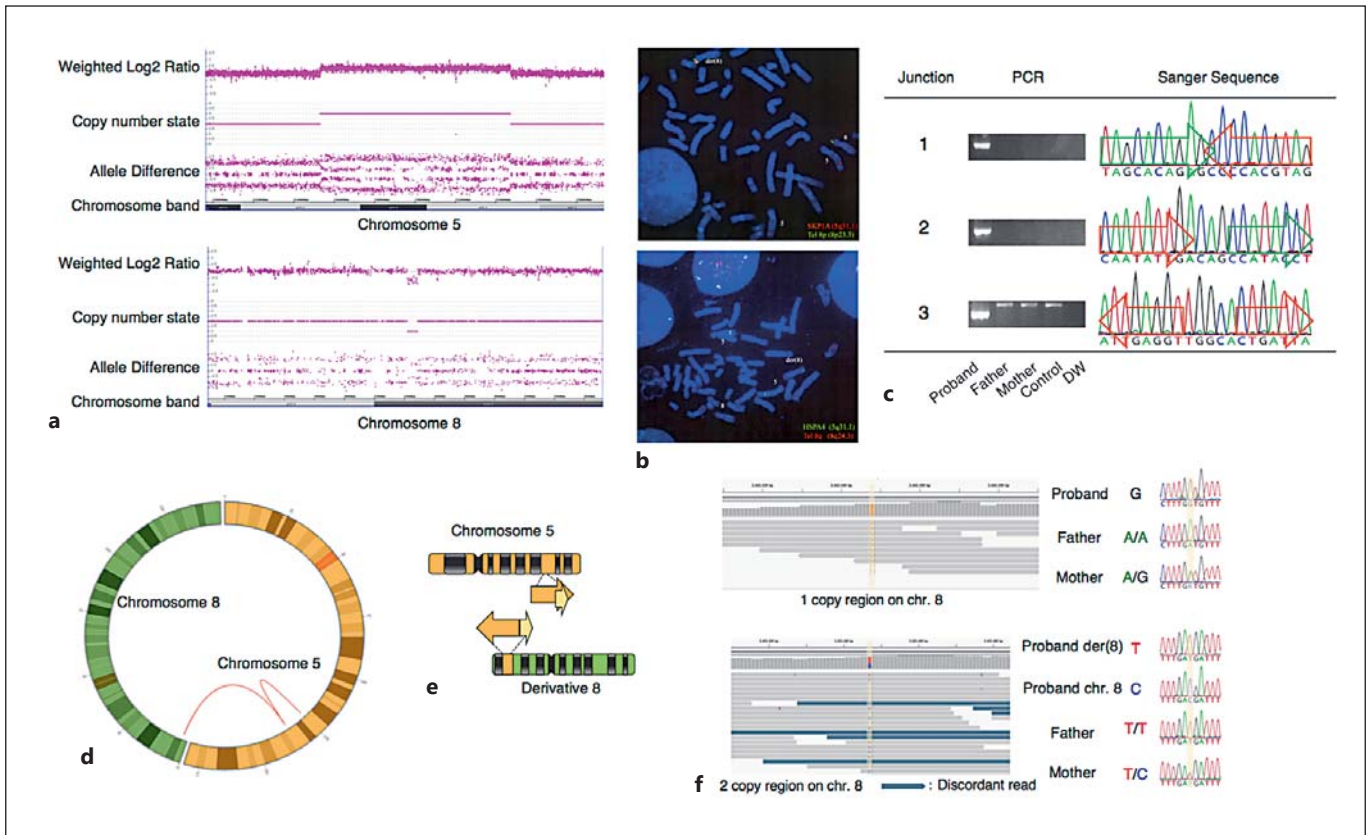


**Fig. 2.** Analysis of the chromosomal insertion in case 2. **a** Copy number abnormalities in chromosomes 5 and 8 are graphically displayed using ChAS. Positional information on the copy number change is designated as  $\text{arr}[\text{hg}19] \ 5\text{q}23.2\text{q}31.1(125,311,267\text{--}134,731,795)\times 3,8\text{p}23.2(2,421,059\text{--}2,488,315)\times 1$ . **b** FISH analysis confirming the insertion of 5q31.1 (red) into the vicinity of 8p23.3. **c** Breakpoint-specific PCR and its sequence. The analysis was performed as described in Figure 1. Orange and green arrows indicate chromosomes 5 and 8, respectively. The distance between the arrows corresponds to microhomology or microinsertion. **d** The de-

tected chromosomal rearrangements are visualized by a Circos plot using ClicO FS. **e** Two segments in chromosome 5 were shuffled and translocated into chromosome 8. One segment completely overlaps another segment. **f** SNP-based parental origin determination. The top shows the 1-copy region in chromosome 8, whereas the bottom shows the 2-copy region in chromosome 8. The details are the same as those provided in Figure 1. Discordant reads are shown in dark blue. SNPs used for analysis are presented on a yellow background.

### Case 2

This case was referred to our facility for the examination of postnatal short stature. Initial G-banding revealed a 46,XX,add(8)(p22) karyotype. Cytogenetic microarray data showed that the patient had both a duplication at 5q23.2q31.1 and a deletion in chromosome 8p23.2 (Fig. 2a). FISH analysis showed that the interstitial chromosome 8p23.2 deletion was due to an insertion at chromosome 5q23.2q31.1 (Fig. 2b). This insertion was not identified in either of the parents and was thus determined to have occurred de novo in the index case.

To identify the deletion and insertion breakpoints, we applied LUMPY to the whole genome sequencing data. Three breakpoints were found and validated by PCR and Sanger sequencing. One breakpoint was between the 5q regions, while the others were re-joined between chromosomes 5 and 8 but with different orientations. The inserted 5q chromosome comprised 2 segments in chromosome 5, one large segment spanning from 125,317,703 to

134,732,368 and the other spanning from 134,730,551 to 134,731,048. This suggests that smaller 497-bp fragments were triplicated and inserted adjacent to the larger insertion in an inverted orientation. Similar to case 1, one junction had a 2-nucleotide microhomology (junction 1), whereas 2 junctions had microinsertions of an unknown origin (Fig. 2c; junctions 2 and 3). The likely structure is shown in Figure 2d, e.

SNP genotyping of the deleted region in chromosome 8 showed that the paternal chromosome 8p23.2 was deleted and that the normal chromosome 8 was of maternal origin. In addition, the inserted 5q segments originated from the paternal chromosome, suggesting that the paternal fragment from chromosome 5 was integrated into the paternal chromosome 8 (Fig. 2f). However, the inserted 5q segments were different from the normal paternal homologue chromosome, indicating the presence of 2 paternal 5q chromosomes. This suggests that one of the paternal chromosomes 5 was shattered and integrated into the paternal chromo-

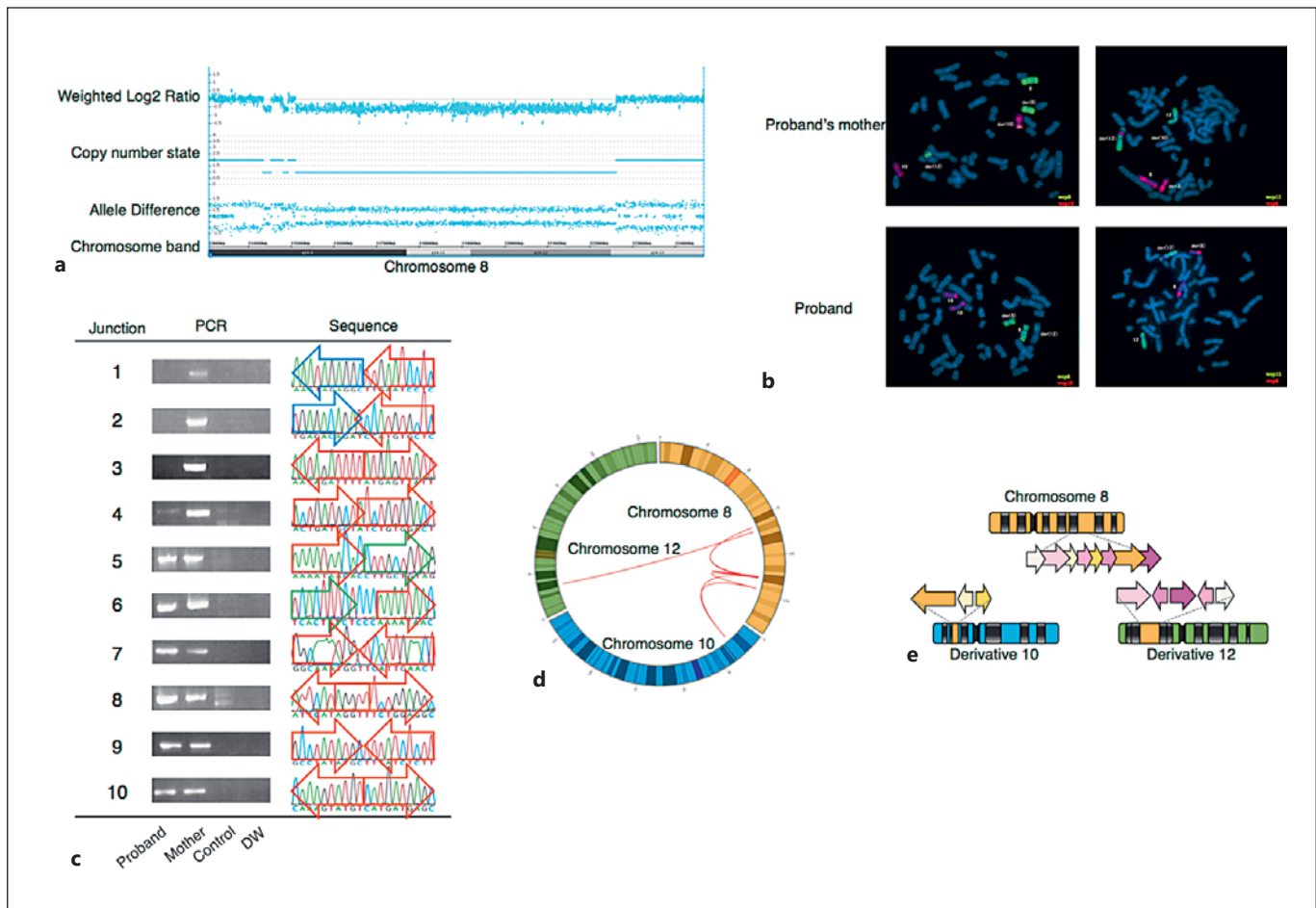


**Fig. 3.** Analysis of the chromosomal insertion in case 3. **a** Analysis of copy number state using ChAS software revealed that the proband had 3 distinct deletions in chromosome 10. The copy number change was designated as  $\text{arr}[\text{hg19}] \ 8\text{q}23.3(114,340,065\text{--}114,527,620)\times 1$ ,  $\text{arr}[\text{hg19}] \ 8\text{q}23.3(114,806,300\text{--}114,925,879)\times 1$ ,  $\text{arr}[\text{hg19}] \ 8\text{q}23.3\text{q}24.13(115,101,169\text{--}122,616,401)\times 1$ . **b** FISH analysis of the proband's mother with whole chromosome painting of chromosomes 8, 10, and 12 confirms the insertion of chromosome 8 into chromosomes 10 and 12. FISH analysis of the proband confirming the insertion of chromosome 8 into chromosome

12. **c** PCR validation of a discordant read. The details are the same as those provided in Figure 1. Orange arrows show chromosome 8, blue arrows show chromosome 10, and green arrows show chromosome 12. The distance between the arrows corresponds to microhomology or microinsertion. **d** The detected chromosomal rearrangements are visualized by a Circos plot using ClicO FS. **e** A number of segments in chromosome 8 were shuffled and translocated into chromosomes 10 and 12. There may be uncharacterized breakpoints in the region of chromosome 8 of the derivative chromosome 12.

some 8p in the premeiotic stage, during MII, or in the postzygotic stage in the trisomic zygote (Fig. 5b).

#### Case 3

This patient was referred to our facility for the diagnosis of Langer-Giedion syndrome. Initial G-banding revealed a  $46,\text{XY},\text{der}(12)\text{ins}(12;8)(\text{p}12;\text{q}21\text{q}23)$  karyotype. CytoScan HD array analysis showed that the proband had a deletion at chromosome  $8\text{q}23.3\text{q}24.13$  (Fig. 3a). The mother of the proband was  $46,\text{XX}$  (data not shown). FISH with whole chromosome painting probe analysis revealed that she had a balanced insertion that involved chromosomes 8, 10, and 12. The long arm of chromosome 8 was found to be inserted into chromosomes 10 and 12. The pro-

band inherited only  $\text{der}(8)$  and  $\text{der}(12)$ , not  $\text{der}(10)$ , resulting in the deletion of chromosome bands  $8\text{q}23.3\text{q}24.13$  and causing Langer-Giedion syndrome (Fig. 3b).

Breakpoint analysis of the chromosomal rearrangements allowed us to identify 10 discordant reads. Of these, 6 junctions were detected in both proband and maternal DNA (junctions 5–10), whereas the remaining 4 were not detected in the proband (junctions 1–4), suggesting that 6 junctions are in  $\text{der}(8)$  and  $\text{der}(12)$ , and 4 are in  $\text{der}(10)$  (Fig. 3c). The inserted chromosome 8 regions consisted of pieces of segments, which were shuffled, rejoined in direct or inverted orientation, and inserted into either chromosome 10 or 12. Six junctions of rearrangements involved simple end-joining (junctions 1, 3, 5, 7, 9, and 10), and the remaining 4

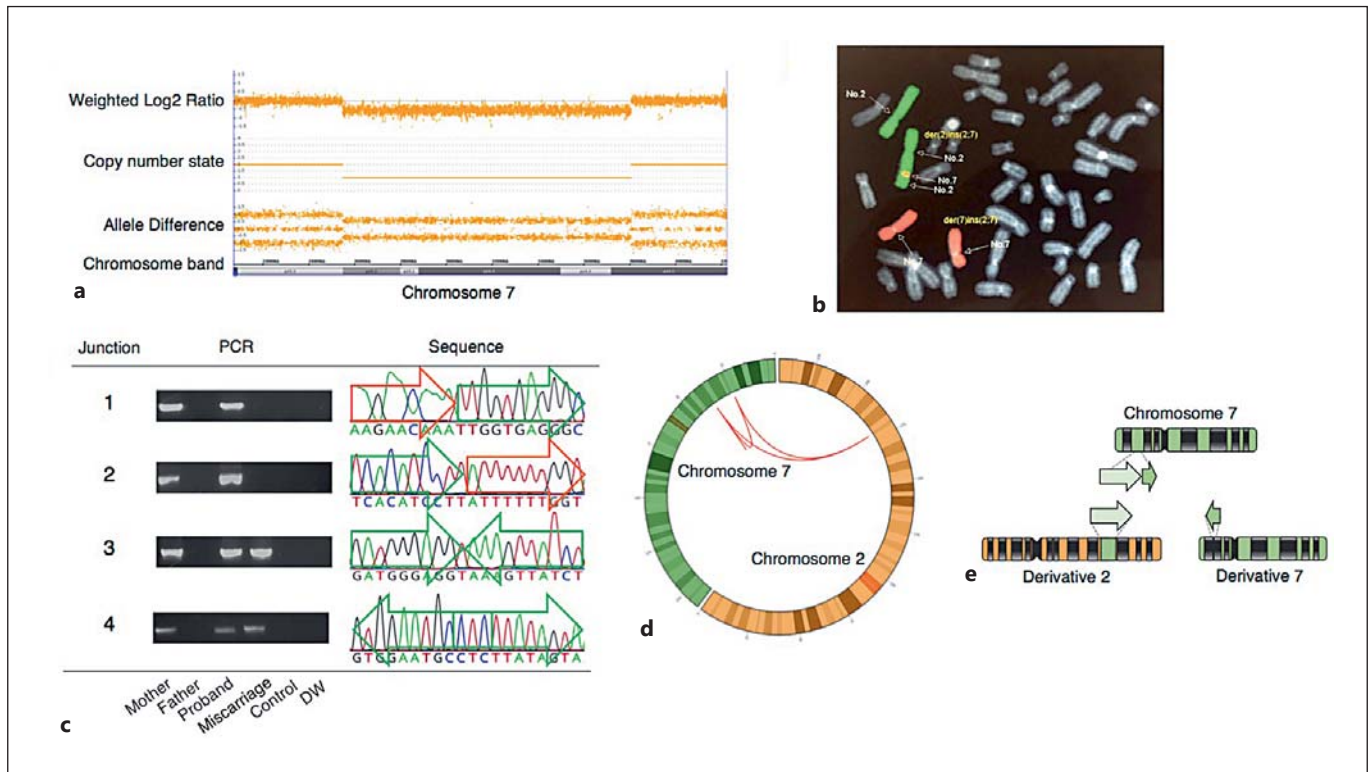


**Fig. 4.** Analysis of the chromosomal insertion in case 4. **a** The fetus has a copy number loss in chromosome 7. The genomic position of the copy number change is arr[hg19] 7p15.3p14.1 (25,471,046–38,067,611)×1. **b** Whole chromosome painting of chromosomes 2 (green) and 7 (red) showing the insertion from chromosome 7 into band 2q. **c** PCR confirmation of a discordant

read. The details are the same as those provided in Figure 1. Orange and green arrows indicate chromosomes 2 and 7, respectively. The distance between the arrows corresponds to microhomology or microinsertion. **d** The detected chromosomal rearrangements are visualized by a Circos plot using ClicO FS. **e** Two pieces of segments in chromosome 7 were inserted into chromosomes 2 and 7.

junctions had either microhomology (junctions 2 and 4) or microinsertion (junction 6). The likely structure is shown in Figure 3d, e.

Because we did not obtain the parental sample of the mother, who was a carrier of a balanced insertion, we could not analyze the origin of the insertion.

#### Case 4

This patient was referred to our facility because of recurrent pregnancy loss. The initial G-banded karyotype was 46,XY,ins(2;7)(q31;p11.2p13). We confirmed the balanced insertion of the proband by whole chromosome painting (Fig. 4b). Cytogenetic microarray analysis revealed that the aborted fetus of the proband had a deletion at 7p15.3p14.1 (Fig. 4a).

Breakpoint analysis of chromosomal rearrangements allowed us to identify discordant reads. Four discordant reads were discovered by LUMPY and validated by junction-specific PCR and Sanger sequencing. Two junctions formed by rejoining between chromosomes 2q and 7p were identified only in the proband, not in the fetus (junctions 1 and 2), whereas the remaining 2 junctions composed of 7p rejoining in an inverted orientation were identified in both the proband and fetus (Fig. 4c; junctions 3 and 4). These results suggest that the fragments of 7p were divided into 2 pieces, one in-

serted into 2q and the other inserted into the same 7p region but in the opposite direction (Fig. 4d). Three were blunt-end rejoined junctions (junctions 1–3) and 1 had a 3-nucleotide microhomology (junction 4). The likely structure is shown in Figure 4d, e.

Junction-spanning PCR showed that the proband's mother also had a balanced insertion. Because we did not obtain samples from the grandparents, we could not analyze the origin of the insertion.

## Materials and Methods

We obtained blood from the patients and their family members. Genomic DNA was extracted using standard procedures. We analyzed 4 patients with an unbalanced chromosomal insertion and their relatives in this study.

### Cytogenetic Analyses of Chromosomal Insertions

Individuals with a chromosomal insertion were identified by FISH and SNP array analysis. FISH analysis was performed on metaphase spreads or interphase nuclei from the patients and their



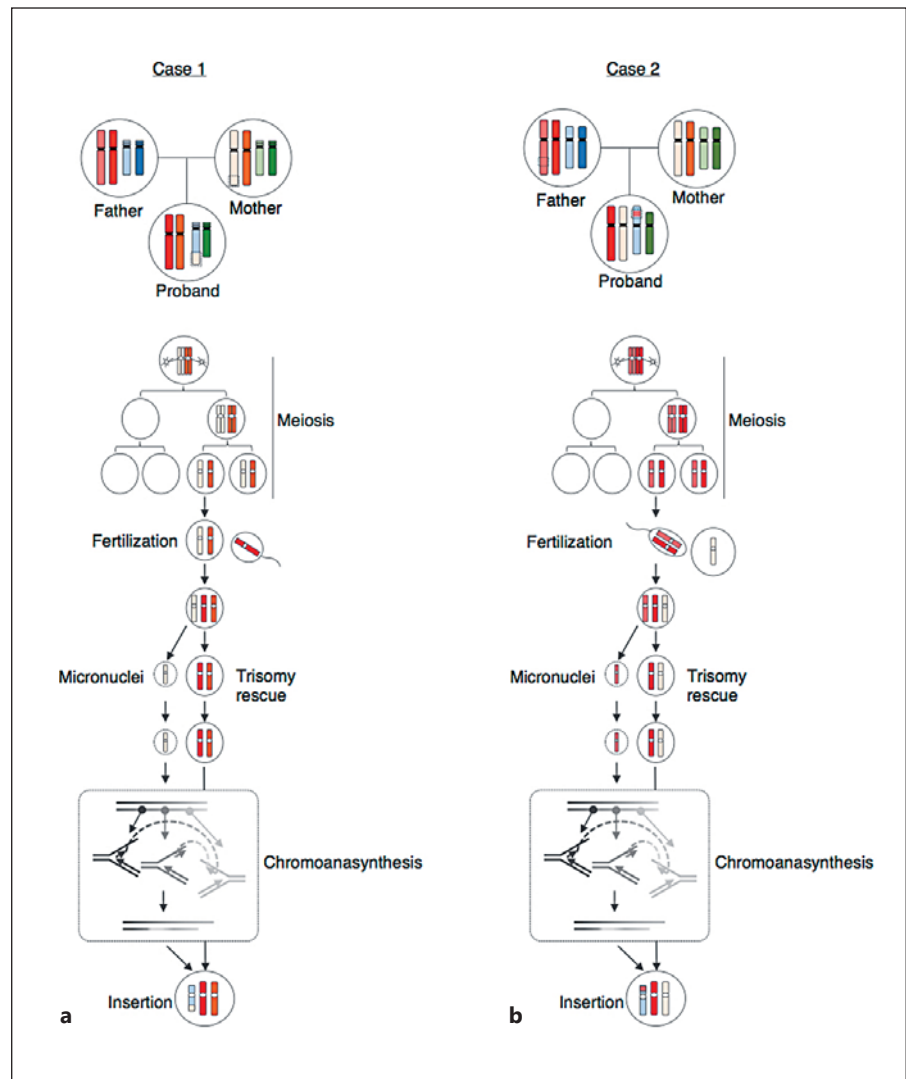


**Fig. 5.** The parental origin of chromosomal rearrangements reveals the mechanism of chromosomal insertion. Parent-of-origin analysis diagrams are shown at the top. Each chromosome is shown in a different color. A trisomic chromosome resulting from malsegregation in meiosis was corrected by subsequent anaphase lagging during an early embryonic stage.

parents, obtained by standard protocols using appropriate region-specific probes and whole chromosome painting probes. SNP array was performed using a CytoScan HD Array Kit (Affymetrix, Santa Clara, CA, USA) for high-resolution analysis of copy number variations and determination of the genotypes of derivative chromosomes. The genome coordinates were based on hg19 in this manuscript.

#### *Breakpoint Characteristics of Chromosomal Insertions by Next-Generation Sequencing*

Mate-pair or paired-end whole genome sequencing was performed to detect the breakpoints of chromosomal rearrangements. Libraries were prepared using a Nextera Mate Pair Library Preparation Kit or TruSeq DNA PCR-Free Library Preparation Kit (Illumina, San Diego, CA, USA) according to the manufacturer's protocol. For preparation of the mate-pair library, fragments of 9 kb in length were extracted. Libraries for next-generation sequencing analysis were then subjected to  $2 \times 100$ -bp paired-end sequencing on a HiSeq 1500 platform (Illumina). Se-

quence data were demultiplexed using bcl2fastq-1.8.4 (Illumina). In the mate-pair sequence case, duplex reads were trimmed using NxTrim [O'Connell et al., 2015]. Sequence reads were then mapped onto the human reference hg19 using BWA 0.7.10 [Li and Durbin, 2010]. Sorting and recalibration of the mapped reads were done using SAMtools 0.1.19 and GATK 3.3-0 [Li et al., 2009; McKenna et al., 2010]. LUMPY was used to identify putative breakpoints of chromosomal rearrangements [Layer et al., 2014]. We focused on discordant reads in the vicinity of the breakpoint junction from FISH and SNP array information. All putative breakpoints were confirmed by visual inspection using the Integrative Genomics Viewer and breakpoint-spanning PCR [Thorvaldsdóttir et al., 2013]. The detected structural variants were visualized by a Circos plot using Ciclo FS [Cheong et al., 2015]. PCR was performed with appropriate primer sets and conditions using TaKaRa Ex Taq DNA polymerase (Takara Bio, Otsu, Japan). Sanger sequencing of breakpoint-spanning PCR fragments was carried out using an ABI3130xl sequencer (Life Technologies, Foster City, CA, USA).

### *SNP-Based Parental Origin Determination*

To determine the parental origin of the chromosomal rearrangement, genotype information from derivative chromosome-specific PCR, SNP array, or whole genome sequencing was compared with that of the parental genotype.

## **Discussion**

In this study, we analyzed chromosomal insertions in 4 individuals. We found that the chromosomal insertions in all 4 cases were not generated by simple inaccurate repair of 3 DSBs, but showed structural complexity. Many pieces of genomic fragments derived from a highly localized chromosomal region were reconstructed in a disorderly array associated with copy number alterations. A recent study of 6 insertion cases also showed similar results [Gu et al., 2016]. The insertion of similar highly shuffled chromosomal segments was also documented in another subset of CSRs, namely, unbalanced translocations [Weckselblatt et al., 2015]. Thus, CSRs, even when observed as a simple rearrangement in conventional karyotyping, are actually more complex than we thought.

Such localized complex CSRs have been termed chromoanagenesis [Holland and Cleveland, 2012; Zhang et al., 2013]. Chromoanagenesis includes 2 different concepts, chromothripsis and chromoanasythesis. Chromothripsis is a local chromosome shattering and restitching by NHEJ, whereas chromoanasythesis is a replication-based complex rearrangement that involves fork-stalling and template-switching as well as microhomology-mediated break-induced replication [Zhang et al., 2009; Kloosterman et al., 2011; Stephens et al., 2011]. Our data show that chromosomal insertions include regions of more than 4 copies in diploid cells, which is not compatible with the definition of chromothripsis (an alteration of 2 copy number states), but rather implies the involvement of a replication-mediated complex rearrangement mechanism. On the other hand, junction analysis showed that the junctions were blunt ended or with short microhomologies or short microinsertions in junction sequences. This conversely implicates the involvement of NHEJ, which is a characteristic of chromothripsis. Given that micronucleus-related chromosome shattering is a mechanism for the origin of chromothripsis, chromosome replication in the micronucleus is not synchronous with that in the nucleus, suggesting that a variable copy number is acceptable in chromothripsis [Crasta et al., 2012; Ly et al., 2017]. Thus, this micronucleus-related chromothripsis pathway may possibly be the mechanism that leads to chromosomal insertion.

Determination of the parental origin of a de novo insertion can shed light on the timing and mechanisms of its formation. In general, de novo constitutional structural rearrangements are predominantly of paternal origin [Thomas et al., 2010]. However, we showed compound paternal and maternal rearrangements in case 1, suggesting a postzygotic origin of the insertion. Such postzygotic CSRs of both parental chromosomes are also observed in de novo unbalanced translocations [Robberecht et al., 2013]. Furthermore, surprisingly, case 1 may have undergone trisomy rescue in the postzygotic stage as evidenced by the presence of 2 maternal and 1 paternal chromosomes. Even in case 2, the presence of 2 paternal chromosomes suggested that the insertion may have arisen in the premeiotic stage or, possibly, in the postzygotic stage in the trisomic zygote. These data imply that the trisomic fertilization may precede the chromothripsis event and be followed by trisomy rescue in the early postzygotic stage, resulting in insertion. [Conlin et al., 2010; Taylor et al., 2014]. Micronuclei formed from anaphase-lagging chromosomes may predispose a pulverized insertion due to low stringency at the spindle checkpoint in this embryonic stage [Mertzanidou et al., 2013]. To conclude, further studies involving higher sample numbers may elucidate a more precise understanding of the mechanisms underlying the etiology of chromosomal insertions.

## **Acknowledgments**

We thank the patients and their families who participated in this study. We also thank Drs. Kazuhiro Matsuda and Masanobu Ito for providing samples as well as Ms. Makiko Tsutsumi, Naoko Fujita, and Asami Kuno for technical assistance. This study was supported by a Grant-in-Aid for Scientific Research from the Ministry of Education, Culture, Sports, Science, and Technology of Japan (15K19042 to T.K., 15H04710 and 24390085 to H.K.) and from the Ministry of Health, Welfare and Labor (16ek0109067h0003 to H.K.).

## **Statement of Ethics**

This study was approved by the Ethical Review Board for Human Genome Studies at the Fujita Health University. Written informed consent was obtained from the patients. All experiments were carried out in accordance with the relevant guidelines and regulations.

## **Disclosure Statement**

The authors have no conflicts of interest to declare.



## References

- Cheong WH, Tan YC, Yap SJ, Ng KP: ClicO FS: an interactive web-based service of Circos. *Bioinformatics* 31:3685–3687 (2015).
- Conlin LK, Thiel BD, Bonnemann CG, Medne L, Ernst LM, et al: Mechanisms of mosaicism, chimerism and uniparental disomy identified by single nucleotide polymorphism array analysis. *Hum Mol Genet* 19:1263–1275 (2010).
- Crasta K, Ganem NJ, Dagher R, Lantermann AB, Ivanova EV, et al: DNA breaks and chromosome pulverization from errors in mitosis. *Nature* 482:53–58 (2012).
- Gu S, Szafranski P, Akdemir ZC, Yuan B, Cooper ML, et al: Mechanisms for complex chromosomal insertions. *PLoS Genet* 12:e1006446 (2016).
- Gu W, Zhang F, Lupski JR: Mechanisms for human genomic rearrangements. *Pathogenetics* 1:4 (2008).
- Hermetz KE, Surti U, Cody JD, Rudd MK: A recurrent translocation is mediated by homologous recombination between HERV-H elements. *Mol Cytogenet* 5:6 (2012).
- Holland AJ, Cleveland DW: Chromoanagenesis and cancer: mechanisms and consequences of localized, complex chromosomal rearrangements. *Nat Med* 18:1630–1638 (2012).
- Kang SH, Shaw C, Ou Z, Eng PA, Cooper ML, et al: Insertional translocation detected using FISH confirmation of array-comparative genomic hybridization (aCGH) results. *Am J Med Genet A* 152A:1111–1126 (2010).
- Kato T, Kurahashi H, Emanuel BS: Chromosomal translocations and palindromic AT-rich repeats. *Curr Opin Genet Dev* 22:221–228 (2012).
- Kloosterman WP, Guryev V, van Roosmalen M, Duran KJ, de Bruijn E, et al: Chromothripsis as a mechanism driving complex de novo structural rearrangements in the germline. *Hum Mol Genet* 20:1916–1924 (2011).
- Kurahashi H, Bolor H, Kato T, Kogo H, Tsutsumi M, et al: Recent advance in our understanding of the molecular nature of chromosomal abnormalities. *J Hum Genet* 54:253–260 (2009).
- Layer RM, Chiang C, Quinlan AR, Hall IM: LUMPY: a probabilistic framework for structural variant discovery. *Genome Biol* 15:R84 (2014).
- Li H, Durbin R: Fast and accurate long-read alignment with Burrows-Wheeler transform. *Bioinformatics* 26:589–595 (2010).
- Li H, Handsaker B, Wysoker A, Fennell T, Ruan J, et al: The sequence alignment/map format and SAMtools. *Bioinformatics* 25:2078–2079 (2009).
- Ly P, Teitz LS, Kim DH, Shoshani O, Skaletsky H, et al: Selective Y centromere inactivation triggers chromosome shattering in micronuclei and repair by non-homologous end joining. *Nat Cell Biol* 19:68–75 (2017).
- McKenna A, Hanna M, Banks E, Sivachenko A, Cibulskis K, et al: The Genome Analysis Toolkit: a MapReduce framework for analyzing next-generation DNA sequencing data. *Genome Res* 20:1297–1303 (2010).
- Mertzaniadou A, Spits C, Nguyen HT, Van de Velde H, Sermon K: Evolution of aneuploidy up to Day 4 of human preimplantation development. *Hum Reprod* 28:1716–1724 (2013).
- Neill NJ, Ballif BC, Lamb AN, Parikh S, Ravnani JB, et al: Recurrence, submicroscopic complexity, and potential clinical relevance of copy gains detected by array CGH that are shown to be unbalanced insertions by FISH. *Genome Res* 21:535–544 (2011).
- Nowakowska BA, de Leeuw N, Ruivenkamp CA, Sikkema-Raddatz B, Crolla JA, et al: Parental insertional balanced translocations are an important cause of apparently de novo CNVs in patients with developmental anomalies. *Eur J Hum Genet* 20:166–170 (2012).
- O’Connell J, Schulz-Trieglaff O, Carlson E, Hims MM, Gormley NA, Cox AJ: NxTrim: optimized trimming of Illumina mate pair reads. *Bioinformatics* 31:2035–2037 (2015).
- Ou Z, Stankiewicz P, Xia Z, Breman AM, Dawson B, et al: Observation and prediction of recurrent human translocations mediated by NAHR between nonhomologous chromosomes. *Genome Res* 21:33–46 (2011).
- Robberecht C, Voet T, Zamani Esteki M, Nowakowska BA, Vermeesch JR: Nonallelic homologous recombination between retrotransposable elements is a driver of de novo unbalanced translocations. *Genome Res* 23:411–418 (2013).
- Shaffer LG, Lupski JR: Molecular mechanisms for constitutional chromosomal rearrangements in humans. *Annu Rev Genet* 34:297–329 (2000).
- Stephens PJ, Greenman CD, Fu B, Yang F, Bignell GR, et al: Massive genomic rearrangement acquired in a single catastrophic event during cancer development. *Cell* 144:27–40 (2011).
- Taylor TH, Gitlin SA, Patrick JL, Crain JL, Wilson JM, Griffin DK: The origin, mechanisms, incidence and clinical consequences of chromosomal mosaicism in humans. *Hum Reprod Update* 20:571–581 (2014).
- Thomas NS, Morris JK, Baptista J, Ng BL, Crolla JA, Jacobs PA: De novo apparently balanced translocations in man are predominantly paternal in origin and associated with a significant increase in paternal age. *J Med Genet* 47:112–115 (2010).
- Thorvaldsdóttir H, Robinson JT, Mesirov JP: Integrative Genomics Viewer (IGV): high-performance genomics data visualization and exploration. *Brief Bioinform* 14:178–192 (2013).
- Van Hemel JO, Eussen HJ: Interchromosomal insertions. *Hum Genet* 107:415–432 (2000).
- Weckselblatt B, Rudd MK: Human structural variation: mechanisms of chromosome rearrangements. *Trends Genet* 31:587–599 (2015).
- Weckselblatt B, Hermetz KE, Rudd MK: Unbalanced translocations arise from diverse mutational mechanisms including chromothripsis. *Genome Res* 25:937–947 (2015).
- Zhang CZ, Leibowitz ML, Pellman D: Chromothripsis and beyond: rapid genome evolution from complex chromosomal rearrangements. *Genes Dev* 27:2513–2530 (2013).
- Zhang F, Carvalho CMB, Lupski JR: Complex human chromosomal and genomic rearrangements. *Trends Genet* 25:298–307 (2009).